

Research report

# Ultrastructural characteristics and conduction velocity of olfactory receptor neuron axons in the olfactory marker protein-null mouse

Edwin R. Griff<sup>a,\*</sup>, Charles A. Greer<sup>b</sup>, Frank Margolis<sup>c</sup>, Matthew Ennis<sup>c</sup>,  
Michael T. Shipley<sup>c</sup>

<sup>a</sup>Department of Biological Sciences, University of Cincinnati, ML 0006, Cincinnati, OH 45221-0006, USA

<sup>b</sup>Department of Neurosurgery and Section of Neurobiology, Yale School of Medicine, New Haven, CT 06520, USA

<sup>c</sup>Department of Anatomy and Neurobiology, University of Maryland School of Medicine, Baltimore, MD 21201, USA

Accepted 14 March 2000

## Abstract

Olfactory receptor neuron (ORN) axon diameters and the conduction velocity of the compound action potential along ORN axons were studied in olfactory marker protein (OMP)-null mice and genotypically matched controls. The compound action potential was distinguished from postsynaptic field potentials by its shorter latency, its persistence following application of cobalt or kynurenic acid that blocked postsynaptic responses, and its ability to follow paired-pulse stimulation at 300 Hz. Blockade of the postsynaptic field responses by kynurenic acid indicates that in the mouse, as in the rat, glutamate is the olfactory nerve transmitter. The mean conduction velocity of ORNs in wild-type control mice was  $0.47 \pm 0.19$  (S.E.M.) m/s ( $n=5$ ), similar to the conduction velocity reported for other mammals. The mean diameter of ORN axons in control mice was  $0.202 \pm 0.005$  and  $0.261 \pm 0.006$   $\mu\text{m}$  in the OMP-null mice. This increase in fiber diameter in the OMP-nulls predicts an increase in impulse conduction velocity. However, the mean conduction velocity of OMP-null mice,  $0.38 \pm 0.03$  m/s ( $n=6$ ), was not significantly different from control ( $P>0.1$ ). The conduction velocity predicted by the increase in fiber diameter in OMP-null mice was within the 95% confidence interval of the measured value. Thus, OMP-null ORNs are normal with respect to the conduction velocity of their axons. The number of axodendritic synapses in the glomeruli of OMP-null mice is higher than in congenic wild-type mice. © 2000 Published by Elsevier Science B.V. All rights reserved.

*Themes:* Sensory systems

*Topics:* Olfactory senses

*Keywords:* Olfactory marker protein; OMP; Olfactory receptor neurons; Conduction velocity; Axon diameter; Mouse; Gene targeting; Knock-out

## 1. Introduction

Olfactory marker protein (OMP) is an abundant cytoplasmic protein, whose expression is highly restricted to mature olfactory receptor neurons (ORNs). In rodents, OMP may represent as much as 4% of the ORN cellular protein. The expression of OMP is phylogenetically conserved and it is present in the ORNs of essentially all vertebrate species [10]. The OMP gene has been cloned from mouse, rat, human and *Xenopus* [10,35] and the amino acid sequence is 55% identical between mouse and

*Xenopus*. Nevertheless, the function of OMP remains elusive. To address its function, mice lacking the gene for OMP were generated by targeted-gene deletion and homologous recombination in embryonic stem cells [9]. The absence of the OMP gene and of OMP expression in the OMP-null mice was confirmed by Southern analysis, by immunoblots, and by immunocytochemistry [9].

Histological and immunocytochemical analysis of the olfactory neuroepithelium of the OMP-null mice as well as the development and overt behavior of these mice are normal [9]. However, mice from which the OMP gene has been deleted are compromised in their ability to respond to odor stimuli as monitored electrophysiologically and behaviorally. Electroolfactogram (EOG) recordings from the neuroepithelium of OMP-null mice demonstrate a reduced

\*Corresponding author. Tel.: +1-513-556-9739; fax: +1-513-556-5299.

E-mail address: edwin.griff@uc.edu (E.R. Griff)

peak response magnitude to stimulation with a number of different odorants [9]. In addition, the EOG kinetics are slower for both the onset and decay phases of the response. The defect is further demonstrated when the EOG in the null mice is assessed using multiple odor pulses. In contrast to the wild-type normal mice, the EOG of the OMP-null mice to the second stimulus of a pair is markedly reduced over a range of concentrations. The EOG in OMP-null mice had a delayed onset and a slower recovery to the second stimulus in a pair of odor pulses; the altered response was dependent on both interpulse interval and odorant concentration [9,27]. These results have been observed in OMP-null mice on a mixed 129/SvImJ×C57Bl6/J genetic background [9] and confirmed and extended in OMP-null mice on the congenic 129/SvImJ strain background from which the ES cells were derived (see Ref. [27] and ms. in preparation), demonstrating that the influence of the OMP-null genotype is independent of the background strain on which it is expressed.

The EOG deficit implies that there is, overall, a reduction of neural activity in the olfactory projection to the main olfactory bulb (MOB). Consistent with this, OMP-null animals on the mixed 129/SvImJ×C57Bl6/J genetic background exhibit a reduced expression of bulbar tyrosine hydroxylase (TH) activity in the MOBs [9]. This observation was confirmed in OMP-null mice on the congenic 129/SvImJ strain, although the magnitude of the difference is less, indicating a contribution of genetic background to the phenomenon (see Ref. [27] and ms. in preparation).

TH expression in the MOB neurons is dependent on an intact, functional connection with the ORNs [3–5,13,24,28,34]. Therefore, these results suggest either a decrease in functional activity of ORNs in the OMP-null mice or, fewer ORN synapses onto MOB neurons. In addition, recent behavioral testing of OMP-null animals has demonstrated a 2-log loss of olfactory sensitivity in OMP-nulls [41], further confirming a functional deficit in transduction, transmission, or processing of olfactory information in the OMP-null mice.

To pursue additional potential mechanisms underlying the functional deficit in the OMP-null olfactory system, the present study was designed to assess the status of the olfactory nerve, the connection between the ORNs in the olfactory epithelium and their synaptic targets in the MOB. Specifically, we tested the hypothesis that a decrease in ORN activity/excitability in OMP-null mice was a reflection of either a change in the morphology and/or electrical properties of the ORN axons. To test for a deficit in the functional status of the axonal membrane, the compound action potential was characterized and conduction velocity measured in both OMP-null and wild-type mice. The morphological characteristics of the ORN axons were established using electron microscopy to assess the ultrastructural features of the ORN axons and the synaptology

of the OMP-null and wild-type MOB glomeruli where the ORN axons terminate.

## 2. Materials and methods

### 2.1. OMP-null mice

The generation of the OMP-null line of mice has been described in detail [9]. All the OMP-null mice used in this study were derived by backcrossing the initial chimeric founder with congenic mice of strain 129/SvImJ, the strain background from which the ES cells were derived. The resulting hemizygous mice were bred to achieve a homozygous line of OMP-null mice on the 129/SvImJ background, which was the strain that provided all of the control mice used in this study.

### 2.2. Electron microscopy

Adult male OMP-null ( $n=3$ ) and wild-type controls ( $n=3$ ) were anesthetized with an i.p. administration of 75 mg/kg pentobarbital (Nembutal) and perfused through the heart with 0.1 M phosphate-buffered saline (PBS) (pH 7.2) followed by 4% paraformaldehyde and 1% glutaraldehyde in 0.1 M PBS. The brains were removed and immersion fixed for an additional 24 h at 4°C. Following several rinses in 0.1 M phosphate buffer, the MOBs were processed for routine transmission electron microscopy, as we have previously described [17]. Briefly, following dehydrations through ascending alcohols and a 1-h immersion in 1% alcoholic uranyl acetate, the tissue was embedded in EPON and polymerized at 60°C for 48 h. Transverse thin sections (70–100 nm) were cut from the trimmed EPON blocks and mounted on 1×2 mm formvar-coated slot grids. The sections were examined at 70 kV using a Jeol 1200 electron microscope. Images were captured at an initial magnification of ×10 000 and printed at a final working magnification of ×26 000. All procedures were approved by the Yale University School of Medicine Animal Care and Use Committee (Protocol # 07161).

To obtain an estimate of the diameter of the ORN axons, the maximum diameter of 200 randomly selected axons was measured in both the null and wild-type mice. To obtain an estimate of the number of microtubules in ORN axons, microtubules were counted in a second random population of 200 axons from both the null and wild-type mice. Microtubules were defined by their spherical outline, ~20–25 nm cross-sectional diameter, and the slight patency at their core. They were easily distinguished from the neurotubules, ~10 nm in diameter, found in ORN axons and the cisternae of smooth endoplasmic reticulum, irregular in outline and >50 nm in diameter, which can also be encountered. All axon measurements and microtubule counts were made by blind observers using coded electron micrographs. Measurements are reported as

mean $\pm$ S.E.M.; significance was determined using a Student's *t*-test.

Synapses within the glomerular neuropil were identified based on the polarity of the pre- and postsynaptic membrane specializations, the number and shape of the synaptic vesicles and the shape and electron density of the pre- and postsynaptic profiles [20,23,33]. In both the wild-type and OMP-null mice, 9000  $\mu\text{m}^2$  of glomerular neuropil were examined. Synapses were classified as: (1) ORN axon to dendrite (Gray Type I axodendritic); (2) mitral/tufted dendrite to periglomerular cell dendrite (Gray Type I dendrodendritic); or (3) periglomerular cell dendrite to mitral/tufted cell dendrite (Gray Type II dendrodendritic). All synapse characterizations and counts were made by blind observers using coded electron micrographs.

### 2.3. Compound action potential analyses

Conduction velocity measurements were made on five wild-type and six OMP-null adult male mice weighing  $25.5\pm 4$  and  $26.0\pm 5$  g, respectively. All procedures were approved by the Animal Welfare committee of the University of Maryland. Animals were deeply anesthetized with 4% chloral hydrate (400 mg/kg) and an intraperitoneal tube inserted for supplemental injections (0.02 ml) every 30 min or as needed. The animal was then secured in a stereotaxic apparatus with a snout holder built for a mouse. Core body temperature was maintained at 35°C with a heating pad. The dorsal MOB surface was exposed by drilling a hole in the frontal bone; in some experiments the lateral surface was also exposed through the orbit. The surface of the MOB was kept moist with saline.

A bipolar stimulation electrode was made from a pair of twisted 125- $\mu\text{m}$  stainless steel wires insulated except for the tips. This electrode was positioned at the rostral end of the MOB to stimulate the ORN axons after they passed through the cribriform plate. The recording electrode, a 125- $\mu\text{m}$  stainless steel wire insulated except for the tip, was positioned caudal to the stimulation electrode to record the compound action potential. In some experiments, a glass micropipette (2–3  $\mu\text{m}$  tip diameter) filled with saline penetrated the MOB using a micromanipulator (David Kopf Instruments, Model 650) to record the evoked responses at different depths.

Stimuli were isolated, constant-current, square-wave pulses 50  $\mu\text{s}$  in duration, 100–500  $\mu\text{A}$  (Astromed/Grass Model S8800). The larger currents were needed to evoke responses when the recording electrode was farther from the stimulation electrode. Single stimuli were delivered at 0.5 Hz; paired pulses were delivered with interpulse intervals between 2 and 20 ms. Responses were amplified and displayed using conventional electrophysiological methods [22], digitized (Cambridge Electronic Design, CED1400), and stored on computer. The typical surface response was triphasic with a prominent negative component [30]. *Spike2* software (CED) was used to calculate

the time between stimulus onset and the trough of this negative component.

In some experiments synaptic transmission was blocked to distinguish the compound action potential from other components of the field potential. This was accomplished by bathing the surface of the MOB with saline containing the glutamate receptor antagonist kynurenic acid (KYN, 10 mM) or cobalt chloride (10 mM).

The impulse conduction velocity was calculated from the measured distance between the stimulation and recording electrodes and the latency between stimulation and response. For each animal, measurements were made for at least two distances, and at each distance, at least 10 stimuli were presented. The latency for each response was measured and a mean latency for each distance was calculated. These mean latencies were plotted as a function of the distance and the slope (conduction velocity) determined from a linear regression calculated by a weighted method of determinants [8]. Differences between wild-type and OMP-null mice and between measurements from dorsal and lateral bulb were tested for significance using Student's *t*-test.

## 3. Results

### 3.1. Ultrastructural properties of the olfactory nerve

As shown in Fig. 1A,B, the ORN axons in the OMP-null and wild-type mice did not differ qualitatively and were equivalent with prior descriptions (e.g. Refs. [11,19]). At high magnification it is apparent that the axoplasmic organization of the axons from the two strains of mice is equivalent. Mitochondria, smooth endoplasmic reticulum, neurotubules and microtubules were easily identified (Fig. 1A,B). At lower magnification, the individual axons were organized into fascicles (mesaxons) that were surrounded by the processes of ensheathing cells (not illustrated). There was no overt evidence of a pathology in the ORN axons of the OMP-null mice.

### 3.2. Synaptology of the OMP-null glomerulus

Three stereotyped patterns of synaptic connections were observed in the MOB glomeruli of the OMP-null mice. These were consistent with numerous prior descriptions of the synapses found in MOB glomeruli [20,23,33,40]. The axodendritic synapses from the ORN axon terminals onto dendritic processes were abundant (Fig. 1C). The ORN terminal was recognized from their very electron-dense appearance, numerous small, clear, spherical vesicles and the asymmetry of the postsynaptic membrane specialization in the dendrite. The remaining ultrastructural features of these synapses were unremarkable and did not show evidence of any overt pathology. Also, readily identified in the glomeruli were the dendrodendritic synapses that

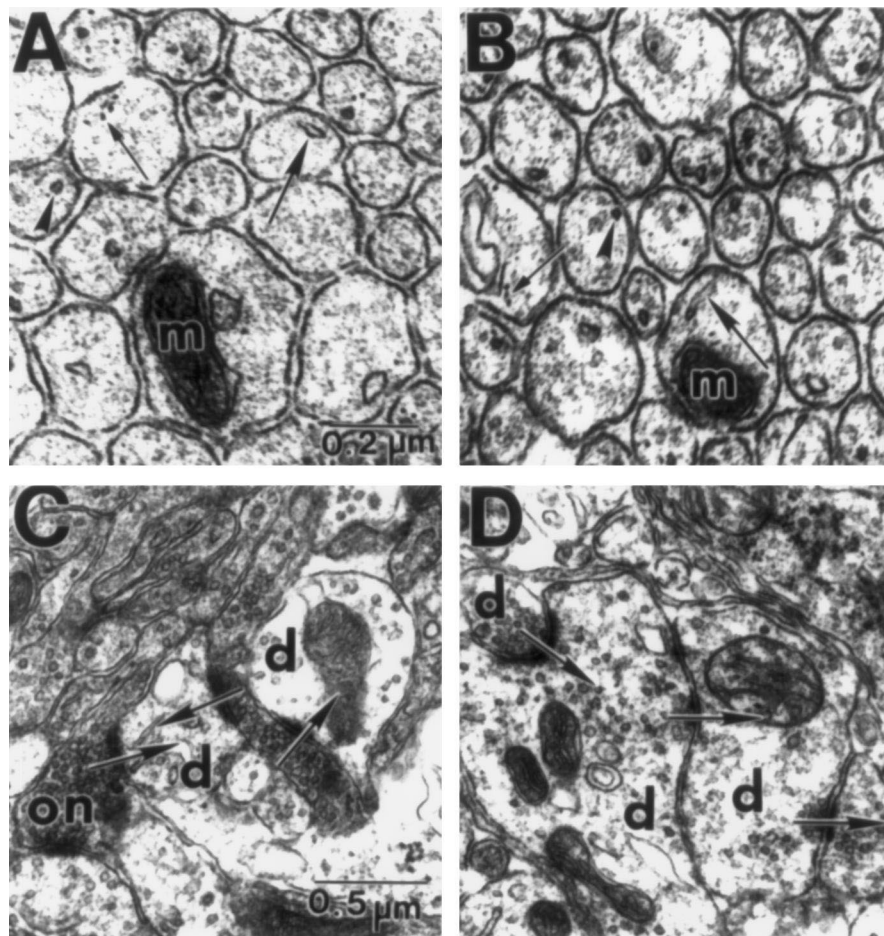


Fig. 1. Electron micrographs of ORN axons from OMP-null and wild-type mice (A,B) and the synapses found in the olfactory bulb glomeruli of OMP-null mice (C,D). In (A) and (B) clusters of neurofilaments (small arrows), microtubules (arrowheads) and smooth endoplasmic reticulum (large arrows) are apparent in the transversely sectioned axons. Examples of mitochondria (m) are also present. In (C) axodendritic synapses from ORN axons (on) onto dendritic processes (d) are seen. The polarity of the synapse is indicated with arrows. In (D) a series of dendrodendritic synapses between dendritic processes (d) are seen. Both Gray Type I synapses, upper left and lower right, as well as Gray Type II synapses, center, are shown. The arrows indicate the polarity of the synapses.

establish the local circuits between mitral/tufted and periglomerular cell dendrites (Fig. 1D). The Gray Type I mitral/tufted to periglomerular cell synapse is characterized by a small collection of small, spherical, clear vesicles closely apposed to the presynaptic membrane in the mitral/tufted cell dendrite. The apposing membrane in the periglomerular cell is marked by the asymmetry of its specialization. The accompanying Gray Type II synapse from the periglomerular cell dendrite to the mitral/tufted cell dendrite, which occasionally could be seen as a reciprocal pair, was equally distinctive. The periglomerular cell dendrite exhibited a somewhat larger collection of pleomorphic vesicles while the apposed membrane specialization of the mitral/tufted cell was symmetrical. As noted above, these characteristics were consistent in both the OMP-null mice and the wild-type mice as well as with the prior descriptions of glomerular synaptology.

### 3.3. Quantitative analyses of the ORN axons and glomerular synaptology

To test for possible quantitative alterations in the ultrastructural organization of the olfactory nerve we measured the diameters of the ORN axons in OMP-null and wild-type mice. Because axon diameter is an important determinant of conduction velocity, we reasoned that a change in diameter could contribute to a change in the functional status of the ORN axons. The mean diameter of the ORN axons of the OMP-null mice was significantly larger than in the wild-type mice ( $P < 0.001$ ; OMP-null =  $0.261 \pm 0.006 \mu\text{m}$ ; wild-type =  $0.202 \pm 0.005 \mu\text{m}$ ). Because this could reflect a differential effect of fixation and possible swelling of the tissue, we also counted the mean number of microtubules in the ORN axons of both lines of mice. The number of microtubules varies as a function of

the diameter of an axon [16]. Therefore, we reasoned that if the larger diameter of the OMP-null axons was accurate, there should also be an accompanying increase in the number of microtubules in the ORN axons of the OMP-null mice. Indeed, ORN axons from OMP-null mice had significantly more microtubules than did the wild-type mice ( $P < 0.001$ ; OMP-nulls =  $1.67 \pm 0.06$ ; wild-type =  $1.29 \pm 0.05$ ). These data suggested that the biophysical properties of the ORN axons in OMP-null mice could also differ and be reflected in perhaps a faster conduction velocity and/or larger amplitude synaptic evoked responses in the MOB.

Using the synaptological characteristics described above, we also established the frequency of the three primary categories of glomerular synapses in both the OMP-null and wild-type mice (Fig. 2). Both the Gray Type I and Gray Type II dendrodendritic synapses occurred at equivalent frequencies in the OMP-null and wild-type mice. However, the axodendritic synapse from the ORN axons onto dendrites occurred at a significantly higher frequency in the OMP-null mice than in the wild-type mice ( $P < 0.05$ ).

#### 3.4. Characterization of the compound action potential in wild-type congenic mice

Bipolar stimulation of the ORN axons evoked a field potential from the surface of the MOB. The initial response following the stimulus artifact was typically triphasic, consisting of a positive–negative–positive sequence, with the negative component largest (see control responses, Fig. 3A,B); following this initial response was a slower negativity. To demonstrate that the initial triphasic component was generated presynaptically by the ORN axons

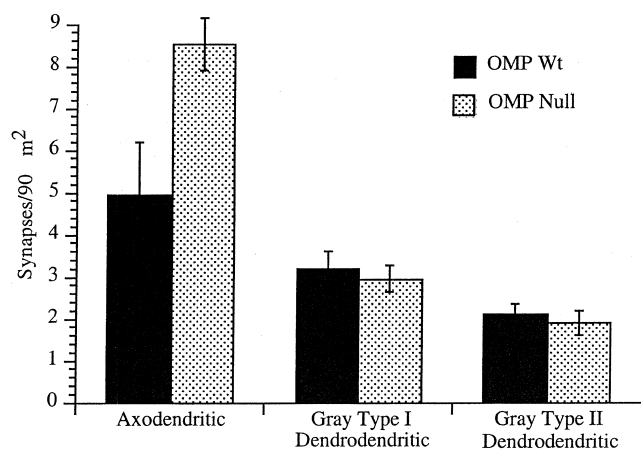


Fig. 2. Mean ( $\pm$ standard error of the mean (S.E.M.)) number of axodendritic, Gray Type I dendrodendritic (mitral/tufted to periglomerular) and Gray Type II (periglomerular to mitral/tufted) dendrodendritic synapses in the glomeruli of OMP-null and wild-type mice. Calibration bar shown in (A) for (A) and (B); shown in (C) for (C) and (D).

and that the slower component was generated postsynaptically by bulbar neurons, blockers of synaptic transmission were applied to the surface of the MOB.

Cobalt has been shown to block synaptic transmission at the neuromuscular junction [39] and in the retina between photoreceptors and horizontal cells [18,31]. Fig. 3A shows that application of 10 mM cobalt to the surface of the bulb abolished the slower, more sustained negative component without affecting the initial triphasic response. When the cobalt was washed out by flushing the surface with saline, the slower negative response recovered.

Postsynaptic responses can also be blocked by antagonists. In the rat and turtle ORNs make excitatory, glutamatergic synapses with mitral cells in the glomerular layer of the MOB [2,7,14]. Fig. 2B shows that the nonselective ionotropic glutamate receptor antagonist kynurenic acid (KYN) eliminated the slow, sustained negative component, but did not significantly alter the initial triphasic potential. When the antagonist was washed out, the slower component recovered. Since the initial triphasic response was spared by both a presynaptic and postsynaptic blocker of synaptic transmission, it was identified as the compound action potential propagating along ORN axons.

Evoked responses were also recorded at different depths in the MOB. At and/or near the surface, the response recorded with a glass micropipette is similar to the control responses described above. As the pipette was advanced into the bulb, the initial triphasic response disappeared, and the slower component increased in amplitude (Fig. 3C). At a depth between 400 and 550  $\mu\text{m}$  from the surface, the slower component reversed polarity, as has been shown previously [29,30]. This depth profile suggested that the compound action potential was recorded from ORN axons as they traversed the MOB in the olfactory nerve layer while the later negative components were due to synaptic activity within the MOB.

Fig. 3D shows responses to paired-pulse stimulation. As the interpulse interval was decreased from 20 to 3 ms the amplitude of the triphasic response evoked by the second stimulus decreased, but only at an interpulse interval between 2 and 3 ms did it become undetectable. Thus, the triphasic response can follow paired-pulse stimulation with 2–3-ms intervals (330–500 Hz), consistent with this response being an action potential with a 2–3-ms absolute refractory period; similar results were seen in rabbit ORN axons [30].

#### 3.5. ORN conduction velocity in wild-type mice

The experiments described above indicate that surface stimulation of the rostral MOB evokes a triphasic compound action potential. Such responses were recorded at several distances from the stimulating electrode and the latency measured to the large trough of each response. Mean latency at each distance was plotted as a function of

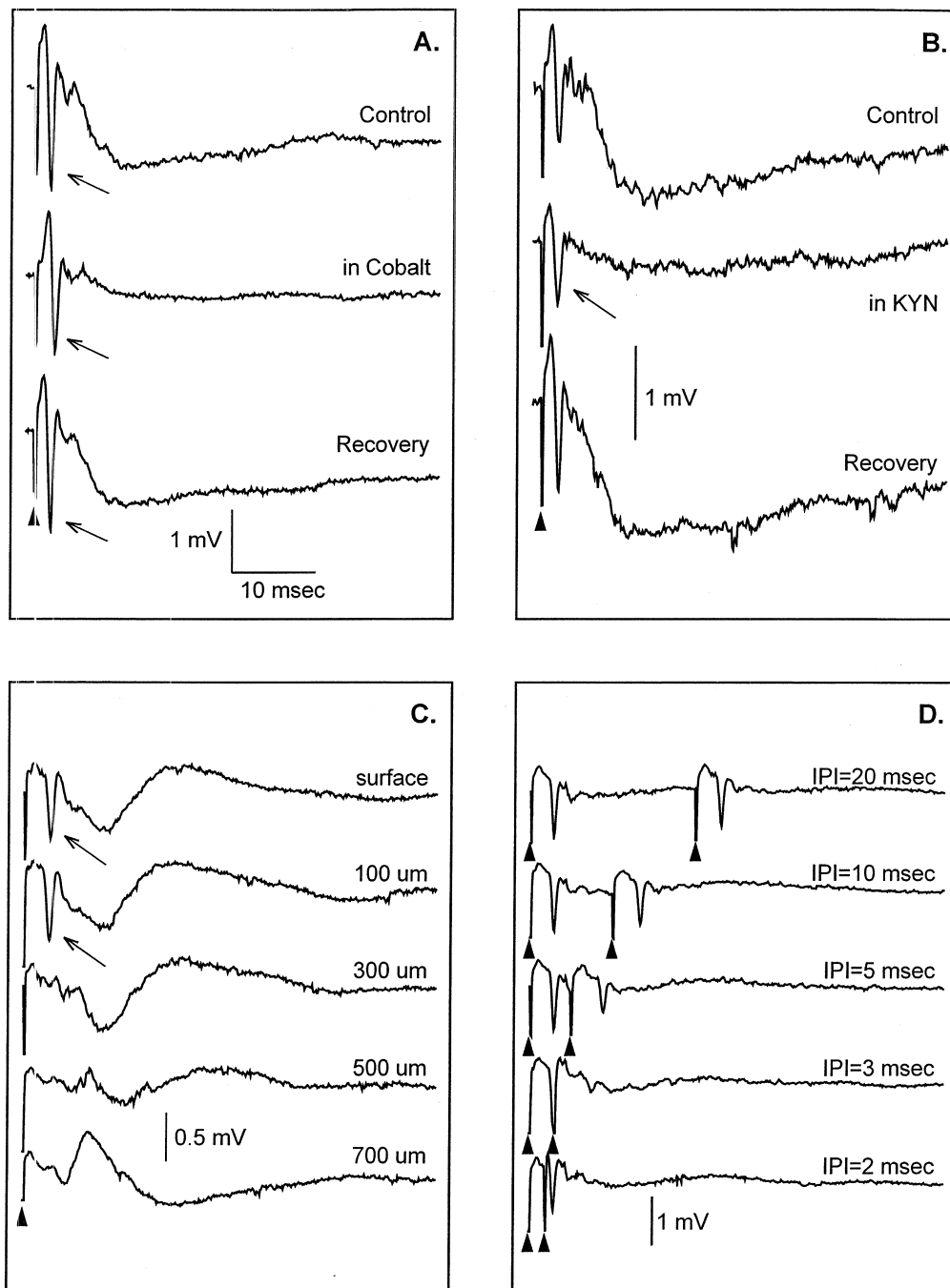


Fig. 3. Identification of the compound action potential in wild-type mice. (A) Effects of cobalt. In the control response, electrical stimulation (filled arrowhead) evokes a stimulus artifact, followed by a triphasic response with a prominent trough (arrow), followed by a slow negativity. 10 mM cobalt chloride, applied to the bulb surface for 6 min, abolished the slow negativity but spared the triphasic response (arrow). After the cobalt was washed out by rinsing with saline for 6 min, the slow negativity that follows the triphasic response (arrow) recovered. (B) Effects of kynurenic acid (KYN). Control response is similar to the control response in (A). 10 mM kynurenic acid for 8 min abolished the slow negativity but spared the triphasic response (arrow). The control response recovered 15 min after the KYN was flushed with saline. (C) Depth profile. A triphasic response is recorded only at the surface and 100  $\mu\text{m}$  depth (arrows). The slow negativity reverses polarity at a depth of about 500  $\mu\text{m}$ . (D) Paired-pulse stimulation. Stimuli (arrowheads) with different interpulse intervals (IPI) were presented. The second stimulus failed to evoke a triphasic response at an IPI of 2 ms.

distance (Fig. 4); the regression line calculated by a weighted least-squares analysis has a slope of  $0.47 \pm 0.19$  m/s; this slope equals the conduction velocity of ORN axons in control congenic mice of the 129SvIm J strain.

### 3.6. ORN conduction velocity in OMP-null mice

The compound action potential in OMP-null mice was identified by the same criteria used for congenic wild-type

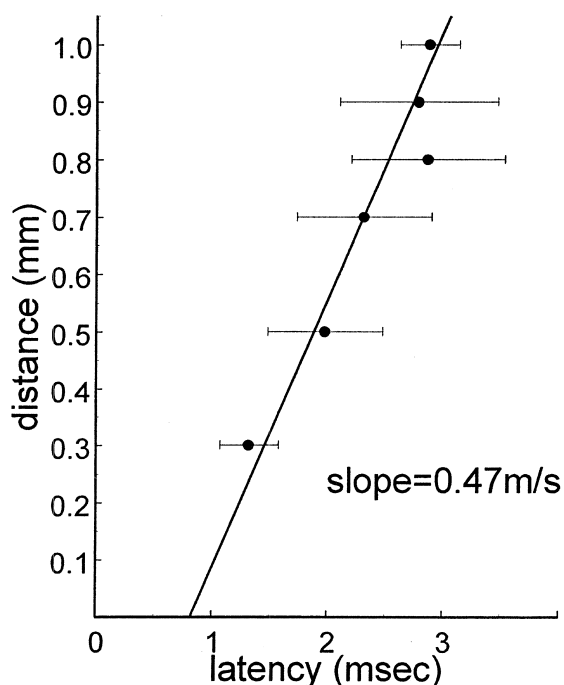


Fig. 4. Conduction velocity of olfactory receptor neurons in wild-type mice. The mean latencies ( $\pm$ standard deviations) of compound action potentials were plotted as a function of the distance between the stimulating and recording electrodes. A linear regression was calculated using the method of weighted determinants; the slope of this line equals the conduction velocity.

mice. Electrical stimulation evoked a field potential at the surface of the MOB consisting of a triphasic potential followed by a slow negativity (Fig. 5A). The triphasic potential was not affected by treatment with kynurenic acid, indicating a presynaptic origin (Fig. 5A). The triphasic response was localized to the superficial 100–150  $\mu$ m of the MOB (Fig. 5B), and had a refractory period of 2–3 ms (Fig. 5C). These results are indistinguishable from those for wild-type congenic mice, and identify this triphasic potential in OMP-null mice as the compound action potential.

Compound action potentials were recorded at several distances from the stimulation electrode, and the latencies measured. Mean latencies at each distance are plotted as a function of distance between the stimulation and recording electrodes (Fig. 6). The linear regression calculated through these data has a slope representing the conduction velocity of the OMP-null mice of  $0.38 \pm 0.19$  m/s. This is not statistically different from the conduction velocity of congenic wild-type mice ( $P > 0.1$ ).

#### 4. Discussion

Our findings demonstrate that while the qualitative features of the ORN axons and the synaptic organization of the glomerulus in OMP-null mice differs quantitatively

from wild-type mice, the impulse conduction velocity of ORN axons suggests that the impulse conduction and refractory properties of the axonal membrane are not discernibly affected.

The ultrastructural appearance of both the ORN axons and the glomeruli were normal in OMP-nulls and, indeed, could not be distinguished from wild-type mice. The observation that the local synaptic networks in the glomeruli, the dendrodendritic synapses, occurred at expected ratios and at a frequency similar in both the OMP-nulls and the wild-type mice is consistent with the belief that OMP is restricted to ORNs in the olfactory system. In addition, because the local circuit synapses occurred at a relatively normal frequency, the data suggest that during development there was physiological activity in the olfactory pathway. Prior studies have shown that in the absence of physiological activity, the local circuit synapses in the olfactory bulb fail to develop [6]. However, because Buiakova et al. [9] and Margolis et al. [27] (and ms. in preparation) had reported lower TH expression in the juxtglomerular neurons of the MOB in OMP-null mice, it seemed likely that overall activity is reduced from normal levels.

The appearance of a greater number of ORN axodendritic synapses in the OMP-nulls was not anticipated. In some sensory systems, such as the visual, during early development there occurs a hypertrophy of axonal arbors that is subsequently pruned to adult levels in conjunction with physiological activity [12]. However, in the olfactory system ORN axons target glomeruli with great specificity and do not show evidence of hypertrophy or related arborization that might be suggestive of the formation of supernumerary or nonspecific synapses [25]. It is provocative, however, to note that in wild-type mice OMP expression begins when the ORN axons downregulate their expression of GAP-43 and establish synapses in the olfactory bulb glomeruli [37,38]. When GAP-43 expression is prolonged, the ORN axons continue to grow and branch within the glomerulus [21]. However, mature neurons do not stain for GAP-43 in either OMP-null or in control mice (D.M. Cummings, F.L. Margolis, unpublished observations). Consequently, one plausible suggestion is that in the absence of OMP expression, the rate of down regulation of GAP-43 is altered resulting in an increase in the frequency of ORN axodendritic synapses.

The ORN axons in the null mice were significantly greater in diameter than those in the wild-type mice. We considered the possibility that the measure of axon diameter was an artifact of tissue fixation or other unknown variables. However, increased axon diameter was accompanied by a corresponding increase in the number of microtubules in the ORN nulls. Since the number of microtubules in axons is proportionate to the caliber of an axon [16], our data suggest that the measured increase in OMP-null axon diameter is real. Though the mechanism that may account for the great caliber of the ORN axons in

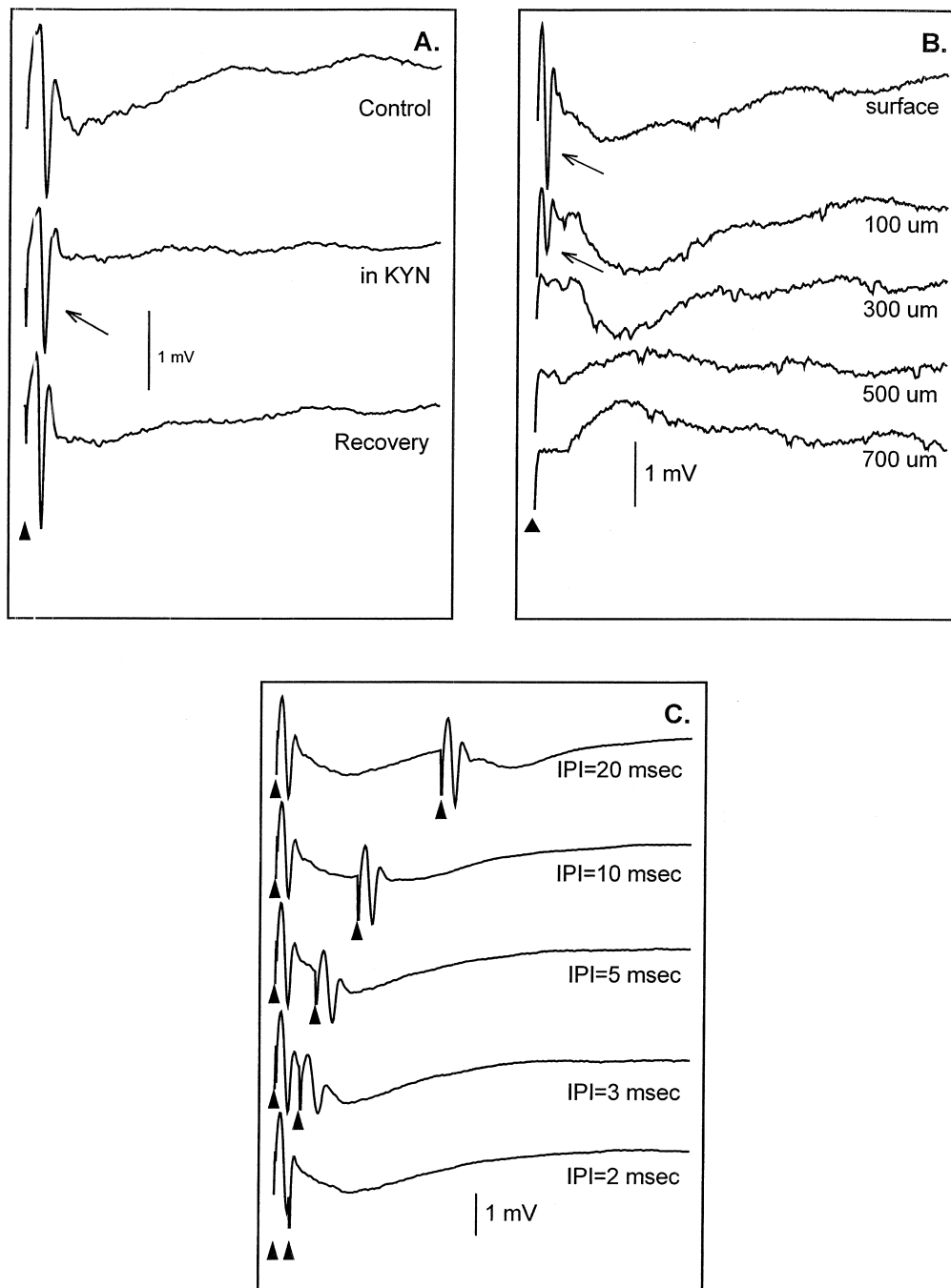


Fig. 5. The compound action potential of OMP-null mice. (A) Effects of kynurenic acid (KYN); KYN applied to the bulb for 3 min abolished the slow negativity, but spared the triphasic potential (arrow). The control response recovered after flushing with saline for 6 min. (B) Depth profile; a triphasic response is recorded only at the surface and 100  $\mu\text{m}$  depth (arrows). The slow negativity reverses polarity at a depth of about 500  $\mu\text{m}$ . (C) Paired-pulse stimulation; stimuli (arrowheads) with different interpulse intervals (IPI) were presented. The second stimulus failed to evoke a triphasic response at an IPI of 2 ms.

OMP-null mice is not known, it prompted the hypothesis that the conduction velocity for action potentials in OMP-nulls would be faster than in the wild-type mice. As discussed below, this was not the case.

The compound action potential is triphasic, follows paired-pulse stimulation at 330–500 Hz, and is recorded only in the superficial layers of the MOB. These results are

similar to those published previously for the rabbit [30]. The conduction velocity of the ORN axons in congenic wild-type mice was calculated from a plot of latency versus distance and found to be  $0.47 \pm 0.16$  m/s. This value is similar to measurements of the ORN axon conduction velocity in rabbit [30], cat [15], opossum [26], and rat [32]. The conduction velocity of the ORN axons in

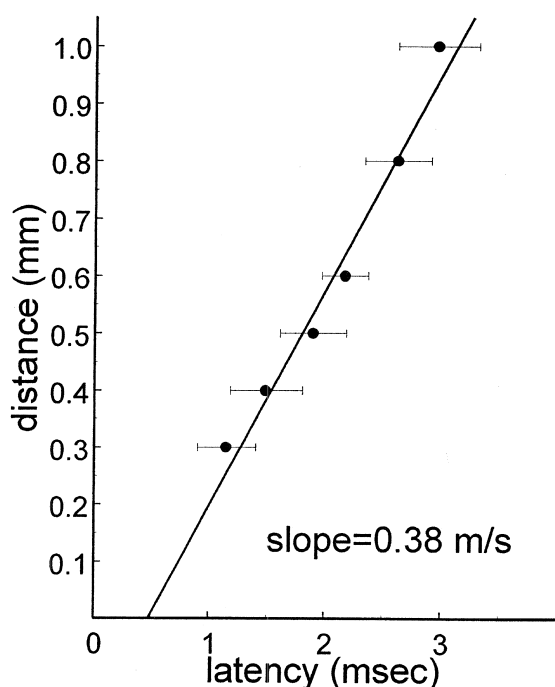


Fig. 6. Conduction velocity of olfactory receptor neurons in OMP-null mice. The mean latencies and standard deviations of compound action potentials were plotted as a function of the distance between the stimulating and recording electrodes. A linear regression was calculated using the method of weighted determinants; the slope of this line equals the conduction velocity.

OMP-null mice was  $0.38 \pm 0.19$  m/s, statistically indistinguishable from congenic wild-type control ( $P > 0.1$ ).

Our impulse conduction velocity measurements would not have detected the faster conduction velocity predicted by the increased ORN axon diameter in OMP-null mice. In unmyelinated axons, such as ORNs, the impulse conduction velocity is proportional to the square root of the axon diameter [1,36]. Using our data for wild-type mice, the proportionality constant is 1.05. The larger ORN axons in OMP-null mice would be predicted to conduct at 0.54 m/s. This predicted faster conduction velocity falls within the 95% confidence interval of the mean conduction velocity of ORNs in OMP-null mice. Thus, the predicted and measured impulse conduction velocities of ORN axons in OMP-null mice are statistically indistinguishable from each other.

These findings show that the impulse conduction velocity of ORN axons in the OMP-null and wild-type mice are indistinguishable. This suggests that the axonal membrane of OMP-null mice is normal, though we cannot exclude the unlikely possibility that there is a compensatory change in the membrane of the OMP-null mutant neurons, so that the conduction velocity does not increase as predicted. The decreased kinetics of the EOG in OMP-null mice therefore probably reflect altered transduction events rather than a general membrane defect. The present results also rule out conduction failure of impulses to the

MOB, and therefore strengthens the hypothesis that OMP plays a role in transduction.

### Acknowledgements

This research was supported by PHS grants DC03195, DC00347, DC02588, DC03112, DC00210, DC03904, NS10174, and NS36940

### References

- [1] D.J. Aidley, in: *The Physiology of Excitable Cells*, Cambridge University Press, London, 1989, pp. 47–49.
- [2] V. Aroniadou-Anderjaska, M. Ennis, M.T. Shipley, Glomerular synaptic responses to olfactory nerve input in rat olfactory bulb slices, *Neuroscience* 79 (1997) 425–434.
- [3] H. Baker, A.I. Farbman, Olfactory afferent regulation of the dopamine phenotype in the fetal rat olfactory system, *Neuroscience* 52 (1993) 115–134.
- [4] H. Baker, T. Kawano, F.L. Margolis, T.H. Joh, Transneuronal regulation of tyrosine hydroxylase expression in olfactory bulb of mouse and rat, *J. Neurosci.* 3 (1983) 69–78.
- [5] H. Baker, K. Morel, D.M. Stone, J.A. Maruniak, Adult naris closure profoundly reduces tyrosine hydroxylase expression in mouse olfactory bulb, *Brain Res.* 614 (1993) 109–116.
- [6] T.E. Benson, D.K. Ryugo, J.W. Hinds, Effects of sensory deprivation on the developing mouse olfactory system: a light and electron microscopic, morphometric analysis, *J. Neurosci.* 4 (1984) 638–653.
- [7] D.A. Berkowicz, P.Q. Trombley, G.M. Shepherd, Evidence for glutamate as the olfactory receptor cell neurotransmitter, *J. Neurophysiol.* 71 (1994) 2557–2561.
- [8] P.R. Bevington, D.K. Robinson, in: *Data Reduction and Error Analysis for the Physical Sciences*, McGraw-Hill, New York, 1992, pp. 96–101.
- [10] O. Buiakova, N.S. Rama Krishna, T.V. Getchell, F.L. Margolis, Human and rodent OMP genes: conservation of structural and regulatory motifs and cellular localization, *Genomics* 20 (1994) 452–486.
- [9] O.I. Buiakova, H. Baker, J.W. Scott, A. Farbman, B. Kream, M. Grillo, L. Franzen, M. Richman, L.M. Davis, S. Abbondanzo, C.L. Stewart, F.L. Margolis, Olfactory marker protein (OMP) gene deletion causes altered physiological activity of olfactory sensory neurons, *Proc. Natl. Acad. Sci. USA* 93 (1996) 9858–9863.
- [11] P.R. Burton, M.A. Wentz, Neurofilaments are prominent in bullfrog olfactory axons but are rarely seen in those of the tiger salamander, *Ambystoma tigrinum*, *J. Comp. Neurol.* 317 (1992) 396–406.
- [12] M. Constantine-Paton, H.T. Cline, E. Debski, Patterned activity, synaptic convergence, and the NMDA receptor in developing visual pathways, *Annu. Rev. Neurosci.* 13 (1990) 129–154.
- [13] M.E. Ehrlich, M. Grillo, T. Joh, F.L. Margolis, H. Baker, Transneuronal regulation of tyrosine hydroxylase mRNA in mouse olfactory bulb, *Mol. Brain Res.* 7 (1990) 115–122.
- [14] M. Ennis, L.A. Zimmer, M.T. Shipley, Olfactory nerve stimulation activates rat mitral cells via NMDA and non-NMDA receptors in vitro, *NeuroReport* 7 (1996) 989–992.
- [15] W.J. Freeman, Spatial divergence and temporal dispersion in primary olfactory nerve of cat, *J. Neurophysiol.* 35 (1972) 733–844.
- [16] R.L. Friede, T. Samorajski, Axon caliber related to neurofilaments and microtubules in sciatic nerve fibers of rats and mice, *Anat. Rec.* 167 (1970) 379–388.
- [17] C.A. Greer, N. Halasz, Plasticity of dendrodendritic microcircuits

- following mitral cell loss in the olfactory bulb of the murine mutant Purkinje cell degeneration, *J. Comp. Neurol.* 256 (1987) 284–298.
- [18] E.R. Griff, Interactions among rods in the isolated retina of *Bufo marinus*, Ph.D. Thesis, Purdue University, West Lafayette, IN, 1979, pp. 77–83.
- [19] N. Halasz, C.A. Greer, Terminal arborizations of olfactory nerve fibers in the glomeruli of the olfactory bulb, *J. Comp. Neurol.* 337 (1993) 307–316.
- [20] J.W. Hinds, P.L. Hinds, Synapse formation in the mouse olfactory bulb: quantitative studies, *J. Comp. Neurol.* 169 (1976) 15–40.
- [21] A.J. Holtmaat, W.T. Hermens, M.A. Sonnemans, R.J. Giger, F.W. Van Leeuwen, M.G. Kapliitt, A.B. Oestreicher, W.H. Gispen, J. Verhaagen, Adenoviral vector-mediated expression of B-50/GAP-43 induces alterations in the membrane organization of olfactory axon terminals in vivo, *J. Neurosci.* 17 (1997) 6575–6586.
- [22] M. Jiang, E.R. Griff, M. Ennis, L.A. Zimmer, M.T. Shipley, Activation of locus coeruleus enhances the responses of olfactory bulb mitral cells to weak olfactory nerve input, *J. Neurosci.* 16 (1996) 6319–6329.
- [23] H.J. Kasowski, H. Kim, C.A. Greer, Compartmental organization of the olfactory bulb glomerulus, *J. Comp. Neurol.* 407 (1999) 261–274.
- [24] T. Kawano, F.L. Margolis, Transsynaptic regulation of olfactory bulb catecholamines in mice and rats, *J. Neurochem.* 39 (1982) 342–348.
- [25] J.R. Klenoff, C.A. Greer, Postnatal development of olfactory receptor cell axonal arbors, *J. Comp. Neurol.* 390 (1998) 256–267.
- [26] P.D. MacLean, B.S. Rosner, F. Robinson, Pyriform responses to electrical stimulation of olfactory fila, bulb, and tract, *Am. J. Physiol.* 189 (1957) 395–400.
- [27] F.L. Margolis, H. Baker, L. Ivic, M. Beinfeld, R. Kream, S. Firestein, O. Buiakova, Influence of genetic background on phenotype of mice with and olfactory marker protein (OMP) gene deletion, *Chem. Senses* 22 (1997) 741.
- [28] N.S. Nadi, R. Head, M. Grillo, J. Hempstead, N. Grannot-Reisfeld, F.L. Margolis, Chemical deafferentation of the olfactory bulb: plasticity of the levels of tyrosine hydroxylase, dopamine and norepinephrine, *Brain Res.* 213 (1981) 365–377.
- [29] W.T. Nickell, M.T. Shipley, Neurophysiology of the olfactory bulb, in: M.J. Serby, K.L. Chobor (Eds.), *Science of Olfaction*, Springer, New York, 1992, pp. 172–212.
- [30] R.A. Nicoll, Olfactory nerves and their excitatory action in the olfactory bulb, *Exp. Brain Res.* 14 (1972) 185–197.
- [31] W.G. Owen, D.R. Copenhagen, Characteristics of the electrical coupling between rods in the turtle retina, in: H.B. Barlow, P. Fatt (Eds.), *Vertebrate Photoreception*, Academic Press, New York, 1977, pp. 169–192.
- [32] S. Phillips, Electrophysiology of the rat olfactory receptor neuron, MS. Thesis, University of Cincinnati, 1998, pp. 62–67.
- [33] A.J. Pinching, T.P.S. Powell, The neuropil of the glomeruli of the olfactory bulb, *J. Cell Sci.* 9 (1971) 347–377.
- [34] A.C. Puche, M.T. Shipley, Odor-induced, activity-dependent trans-neuronal gene induction in vitro: mediation by NMDA receptors, *J. Neurosci.* 19 (1999) 1359–1370.
- [35] P. Rössler, M. Mezler, H. Breer, Two olfactory marker proteins in *Xenopus laevis*, *J. Comp. Neurol.* 395 (1998) 273–280.
- [36] W.A.H. Rushton, A theory of the effects of fibre size in medullated nerve, *J. Physiol.* 115 (1951) 101–122.
- [37] J.E. Schwob, K.E. Mielezko-Szumowski, A.A. Stasky, Olfactory sensory neurons are trophically dependent on the olfactory bulb for their prolonged survival, *J. Neurosci.* 12 (1992) 3896–3919.
- [38] J. Verhaagen, A.B. Oestreicher, W.H. Gispen, F.L. Margolis, The expression of the growth-associated protein B50/GAP43 in the olfactory system of neonatal and adult rats, *J. Neurosci.* 9 (1989) 683–691.
- [39] J.N. Weakly, Action of cobalt ions on neuromuscular transmission in the frog, *J. Physiol.* 234 (1973) 597–612.
- [40] E.L. White, Synaptic organization of the mammalian olfactory glomerulus: new findings including an intraspecific variation, *Brain Res.* 60 (1973) 299–313.
- [41] S. Youngentob, F.L. Margolis, OMP gene causes an elevation in behavioral threshold sensitivity, *NeuroReport* 10 (1999) 15–19.